Interactive comment on “Magnetic dipolarizations inside geosynchronous orbit with tailward ions flow” by Xiaoying Sun et al.

Anonymous Referee #1

Received and published: 31 December 2018

The present paper studied two successive dipolarizations that were observed by the two THEMIS spacecraft located earthward and tailward of the geosynchronous orbit near midnight. These dipolarizations were accompanied by tailward flows. The authors concluded that the tailward flow propagates tailward in a speed of dipolarization region expansion, carrying energy. Before making decision for publication, however, I have a couple of major concerns which require additional data analysis and more detailed discussions.

Responses: We thank you for your comments that help improving the manuscript. In light of your comments, we have revised the manuscript accordingly. Now one-to-one responses are the following.

The authors describe that THEMIS D observed the two successive dipolarizations at _0930 and _0936 UT, while THEMIS E observed only one dipolarization at _0936 UT. The authors associate the two dipolarizations with only one substorm that began at _0930 UT, and they link the dipolarization at THEMIS D at _0930 UT to the dipolarization at THEMIS E at 0936 UT that propagated tailward from the THEMIS D location at a speed of - 47 km/s.

I, however, have a couple of concerns in the above interpretations. First, I am wondering whether the two successive dipolarizations are associated with a substorm or associated with a pseudosubstorm (pseudobreakup) and the following substorm. The authors state that THEMIS D observed the two dipolarizations, but THEMIS E observed only one dipolarization. Ohtani et al. (JGR, p. 19,355, 1993) showed that dipolarization associated with a pseudosubstorm is localized, while that associated with a substorm expands to a wide region. Hence there is a possibility that the _0930 UT dipolarization of the present event is localized at and near THEMIS D, associated with a pseudosubstorm, while the _0936 UT dipolarization expanded to both THEMIS D and E, associated with the following substorm. To verify the interpretation, the authors need to check ground substorm signatures, such as bay-type magnetic field changes, Pi2 and Pi1 pulsations, and auroral activity, at each ground station near the footprints of THEMIS D and E.

Responses: Thank you for this comment. Firstly, there are multiple dipolarizations during a substorm as reported in Paper of Duan et al. 2011 AG（Duan, S. P., Liu, Z. X., Liang, J., Zhang, Y. C., and Chen, T.: Multiple magnetic dipolarizations observed by THEMIS during a substorm, Annales Geophysicae, 29, 331-339, 2011）. The dipolarization at substorm onset is localized with small scale but at substorm enhancement during substorm expansion phase has large spatial scale.

Basing on your suggestions we have checked the ground magnetic field data and present the figures as following. Under the mapping of T96, at 09:30 UT, the footprint of TH-D was near the ground stations of WHIT (White Horse), FSIM (Fort Simpson), ATHA (Athabasca), FSMI (Fort Smith) and LARG (La Ronge); the footprint of TH-E was near the ground stations of ATHA, FSMI, FSIM and

LARG, which are shown in Figure 1'. Figure 2' and Figure 3' provide that the ground magnetic field signatures mark this substorm process as the two dashed vertical lines. The ground stations near the footprints of TH-D and E are listed in Table 1 as following.

Table 1 The geographic longitude, geographic latitude, geomagnetic longitude and geomagnetic latitude of three geomagnetic observatories and satellites, and the local time of these stations at 09:30 UT.

Observatory or satellite	Geographic latitude (°)	Geographic longitude(°)	Geomagnetic latitude(°)	Geomagnetic longitude(°)	09:30 UT ~ LT
TH-D	55.8	233.6	60.4	292.5	01:04
TH-E	55.7	246.4	62.2	307.1	01:57
FSIM	61.8	238.8	65.7	184.6	01:25
FSMI	60.0	248.2	62.4	193.0	02:03
WHIT	61.0	224.8	64.0	279.5	00:29
LARG	55.2	254.7	62.8	317.3	02:29
ATHA	54.7	246.7	57.6	188.1	01:57

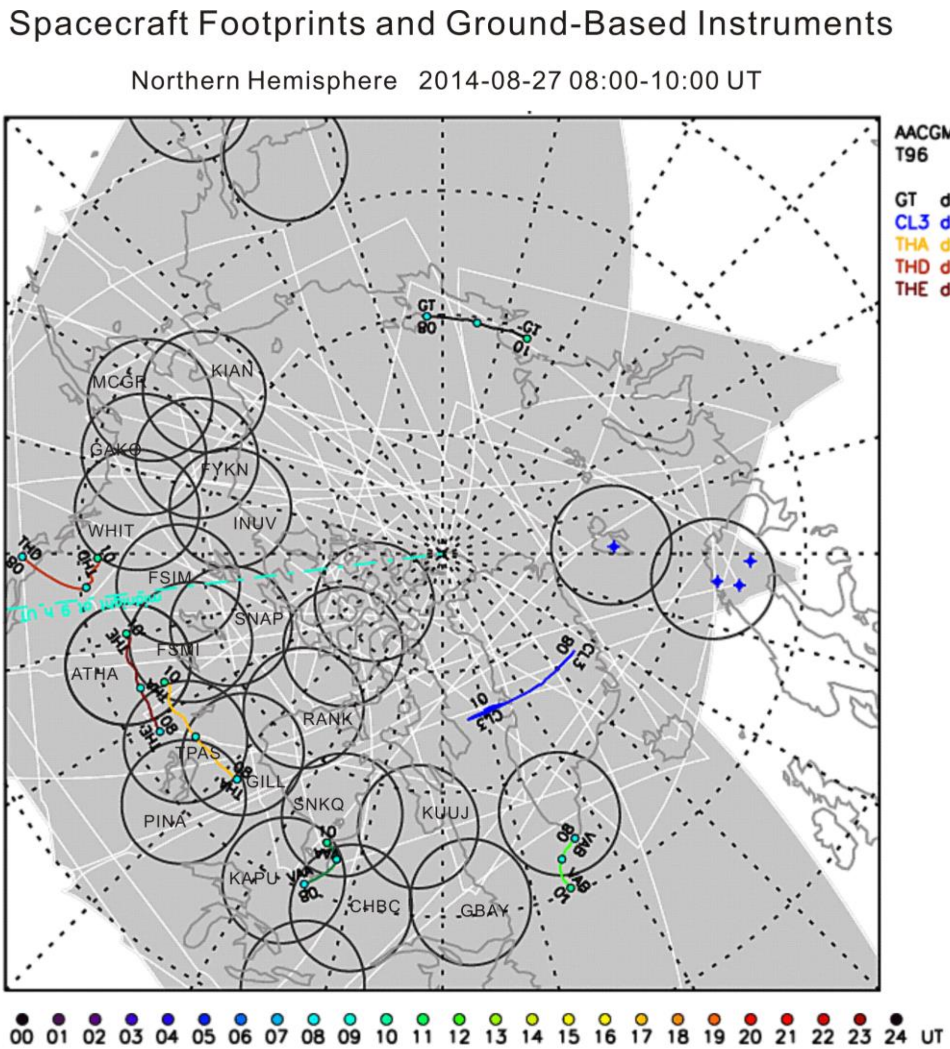

Figure 1' The spacecraft footprints and Ground-Based Observatory.

The 09:30 UT dipolarization is associated with the substorm onset time as marked by the AL index and other ground substorm signatures, such as the bay disturbance and Pi2 plusations as shown in Figure 2’ and Figure 3’. It is not associated with the Pseudosubstorm. This substorm dipolarization is accompanied by the plasma sheet expanding during the substorm expansion phase and propagates toward the magnetotail accompanied by the magnetic field fluctuations with tailward ions bulk flow.

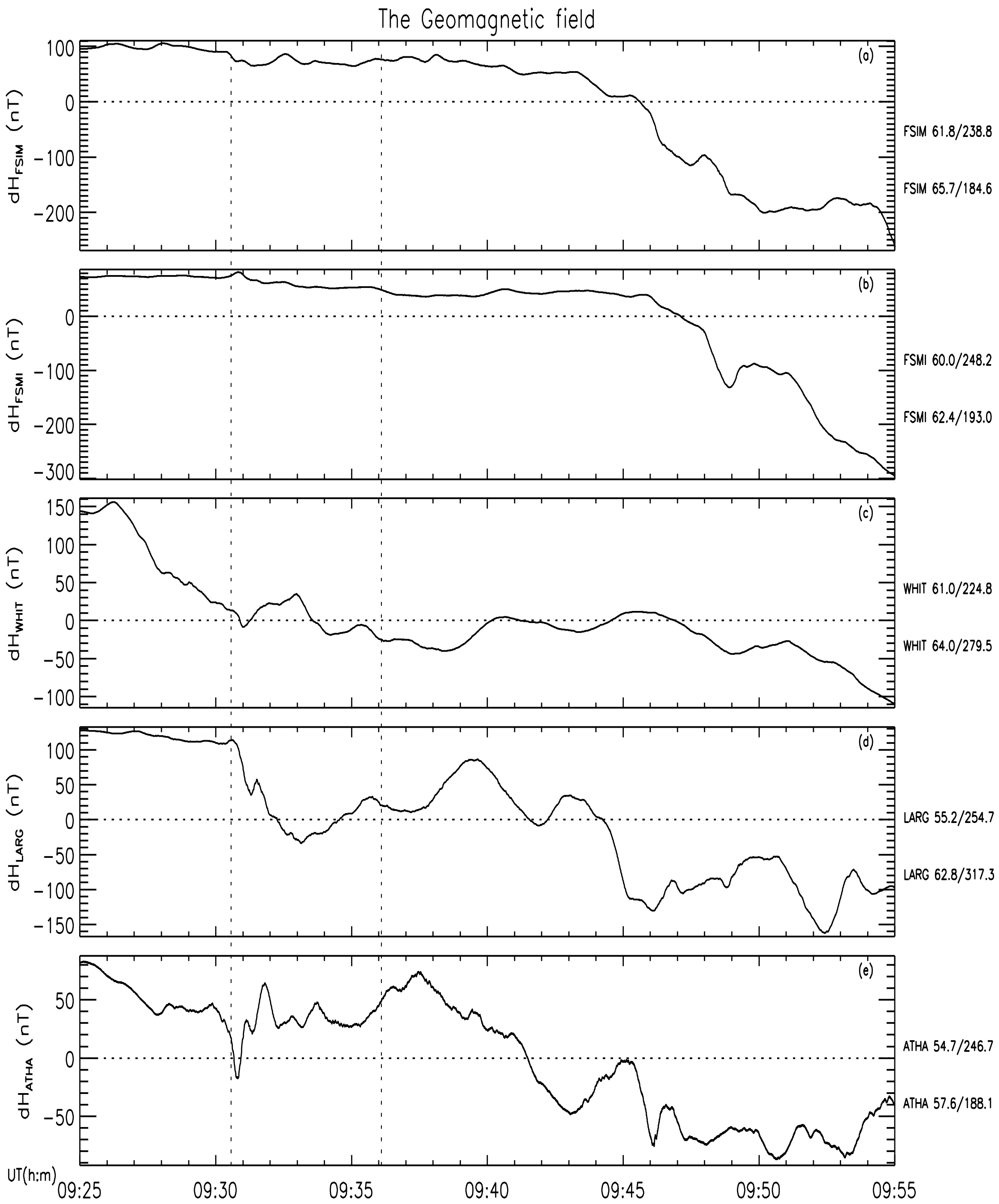

Figure 2’ Geomagnetic field observed by FSIM, FSMI,WHIT, LARG and ATHA between 09:25 UT and 09:55 UT.

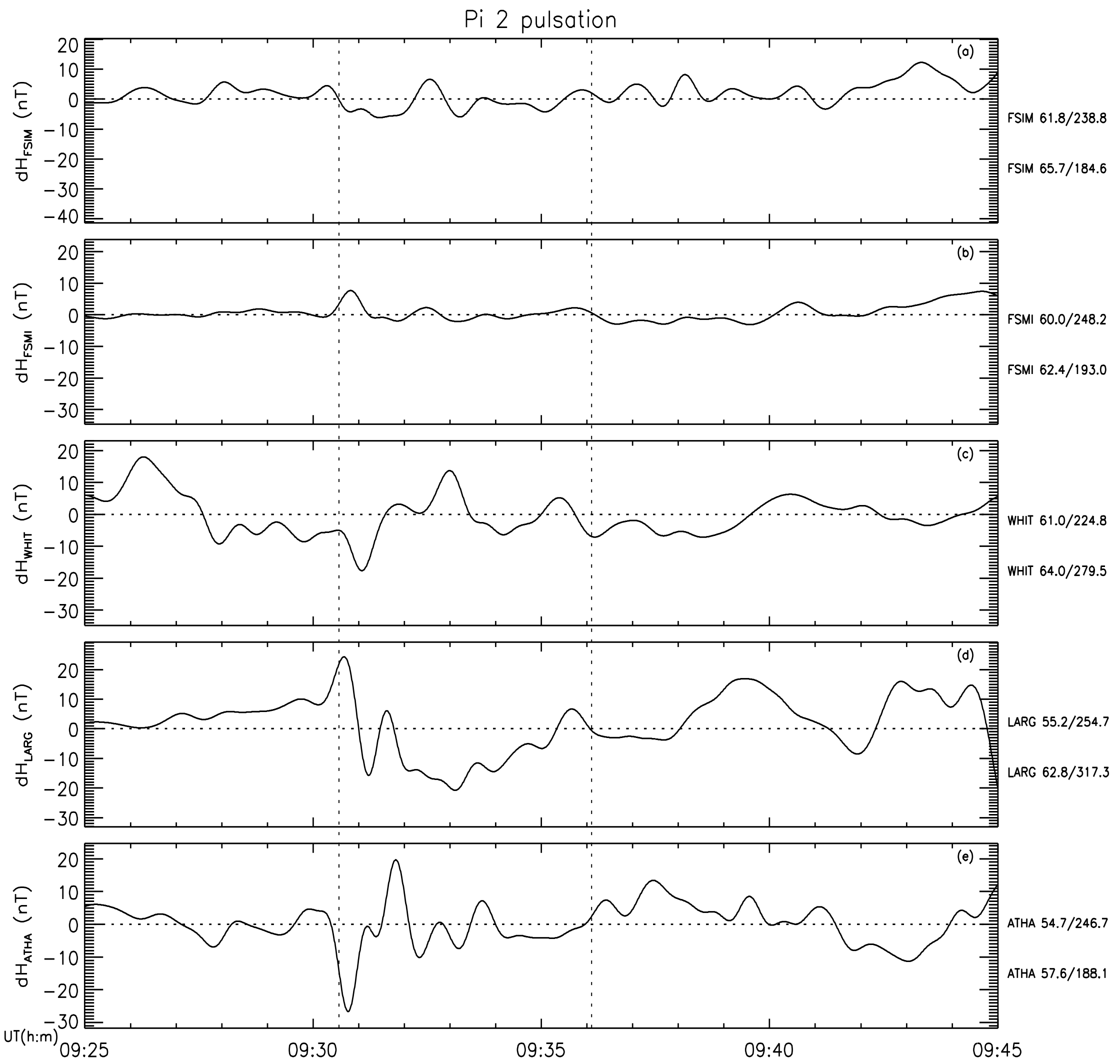

Figure 3’ The Pi 2 observed by FSIM, FSMI, WHIT, LARG and ATHA between 09:25 and 09:55 UT.

On the other hand, at 09:30 UT TH-E is located in the outer magnetosphere, such as in the lobe, the plasma beta and number density are very low. Thus the location of TH-E is far away from the substorm onset region and it cannot detect substorm signatures, such as the magnetic dipolarization.

Ohtani et al. [1993, JGR] reported that the two successive pseudosubstorm during very weak AE index (<100nT) as shown in Figure 2 in their paper. This weak geomagnetic activity was possibly associated with pseudosubstorm. But the geomagnetic activity in our research work is very intense during a moderate storm with AE index being very high ~500nT during our two successive dipolarization. This is a signature of substorms.

At 09:36 UT TH-E is located at the plasma sheet boundary layer. The plasma density and temperature are both increasing, the plasma beta value also increase. These parameters indicated that the near-Earth plasma sheet swept over TH-E spacecraft. This magnetic field elevation angle increases mark near-Earth plasma sheet expansion from the substorm onset location. Thus the dipolarization detected by TH-E at 09:36 UT is associated with the 09:30 UT dipolarization observed by TH-D.

Second, I am wondering whether dipolarization at THEMIS D really occurred in two steps at _0930 and _0936 UT. In Figure 3, it seems that Bz continuously increased from _0930 or _0932 UT through _0937 UT and did not increase stepwise at _0936 UT. Furthermore, THEMIS E observed one dipolarization at _0937 UT. If dipolarization at THEMIS D occurred in two steps and if the dipolarization at THEMIS E is linked to the _0930 UT dipolarization at THEMIS D, how do the authors explain the lack of the second dipolarization at THEMIS E that could be linked to the _0936 UT dipolarization at THEMIS D? The ground signatures mentioned above may be helpful for this question.

Responses: Thank you for this comment. Yes, the Bz component continuously increased from 09:30 UT through 09:37 UT. But it has a sharp increase at 09:36 UT. On the other hand the magnetic field elevation angle θ as shown in Figure 3c also increased sharply at 09:36 UT.

The second dipolarization observed by TH-D at 09:36 UT was also detected by TH-E at 09:41 UT as marked by the third dashed vertical line. Furthermore the energetic electron dispersionless injection, as shown in Figure 5, at 09:30 UT and 09:36UT also supported these dipolarizations inside the geo-synchrounous orbit.

Yes, the ground magnetic field station data as shown above also provide the evidences of these two dipolarizations as shown in Figure 2' and Figure 3'.

After the additional analysis and discussions mentioned above, the dipolarizations at the two spacecraft can be linked, and hence the tailward propagation speed of the dipolarization region can be obtained in a more convincing way.

Responses: Thank you for this comment.

Other specific comments:

Lines 62-67: The maximum AE value of the substorm examined in the present study was _500 nT at _1010 UT, not 1273 nT at a later time. Hence this substorm should be moderate, not intense. After the present substorm, a lot of substorms or steady magnetospheric convection occurred during the storm main phase, and AE reached a peak of 1273 nT during one of these activities.

Responses: Thank you for this comment. We have revised the data in our paper as 'During the main phase of this moderate storm, there is an intense substorm with the AE maximum value ~~1273~~ 700 nT around 10:10 UT' in the line 63.

Line 90: The ion temperature was decreased, not increased, during the weak dipolarization at 0930 UT, while the ion density, the electron density, and the electron temperature were increased. This sentence is confusing, so please reword it.

Responses: Thank you for this comment. We have revised this sentense in our paper as 'The electron density and temperature both increase. The ion density also increases. But ion temperature decreases' in the line 91-92.

Lines 108-109: It should be noted that these low beta values and its increase indicate that the spacecraft was in the lobe and moved to the plasma sheet boundary layer and then the plasma sheet. The parallel flow should have observed in the plasma sheet boundary layer.

Responses: Thank you for this comment. Yes, the parallel flow has observed in the plasma sheet boundary layer which has been mentioned in our paper, lines 110-111: '…the weak dipolarization was with the tailward ions bulk flow, $V_{//}\ x$ ~ -180km/s, is also detected by TH-E around 09:35 UT as shown in Figure 4g'.

Lines 128-129: The negative (tailward) Ex with the positive (northward) Bz corresponds to the duskward perpendicular flow, not the dawnward perpendicular flow. In the present event, the measured Ex is opposite to Ecx calculated from **V**x**B**. The measured electric field may need some caution, since it may include an offset and the contributions other than **V**x**B**.

Responses: Thank you for this comment. Firstly, TH-D is located inside geosynchronous orbit. So the electric field is not dominated by the convection electric field calculated from **V**x**B**. Second, during substorm dipolarization the inductive electric field is significant as shown in Figure 3j. Thus, the detected electric field is different from the convection electric field Ec as shown in Figure 3k.

Lines 143-148: In this paragraph, the authors discuss only the azimuthal speed of the dipolarization region expansion and do not discuss the tailward speed. Since the tailward speed is related to the main conclusion of the present study, it should be discussed as well.

Responses: Thank you for this comment. We have added the discussion of the tailward speed of the dipolarization in our paper line 149 to 153 as 'The dipolarization associated with the current disruption propagated tailward with speed V_x ~ -100 km/s detected by THEMIS satellites in the near-Earth plasma sheet X~ -11 R_E [Liu et al., 2008]. It is larger than the dipolarization propagating speed from inside to outside geosynchronous orbit V_x ~ -47 km/s . The different speeds of dipolarizations propagating tailward imply that the magnitude of the dipolarization speed may be associated with its beginning location in magnetotail plasma sheet.'

Discussion: The current disruption model for substorm triggering proposed that current disruption and dipolarization launches a tailward propagating rarefaction wave, which should be accompanied by a fast earthward flow (e.g., Lui, JGR, p. 1849, 1991; Chao et al., PSS, p. 703, 1977). This is possibly in contrast to the present results. Hence it might be good to discuss this discrepancy or how different the rarefaction wave proposed by the current disruption model and the tailward propagation of the tailward flow and dipolarization region discussed in the present paper.

Responses: Thank you for this comment. The recommended references above have been cited in our paper as in line 155 to 158 'On the other hand, Lui [1991] reported that substorm disturbance propagated tailward through a rarefaction wave front accompanied by earthward flow during substorm expansion phase early period. Chao et al. [1977] proposed that the rarefaction wave propagating tailward was accompanied by the thinning of plasma sheet and earthward plasma flow. This earthward flow is possibly convection flow or outflow flow of magnetic reconnection from the middle magnetotail. '

Minor corrections:

Line 33: NESP –> NEPS

Responses: Thank you for these comments. We have revised the abbreviation as 'NEPS' in the line 33.

Line 35: Liang et al., 2008 –> 2009 ?

Responses: Thank you for these comments. We have revised 'Liang et al., 2008' to 'Liang et al., 2009' in the line 35.

Line 42: Liang et al. (2008) should be deleted here because Liang et al. (2008) did not show magnetotail observations.

Responses: Thank you for these comments. We have revised 'Liang et al., 2008, 2009' to 'Liang et al., 2009' in the line 42.

Lines 60-61: Dst –> Sym-H

Line 61: Figure 1e –> Figure 1f

Responses: Thank you for these comments. We have revised the sentense as 'The minimum value of SYM-H index is about -90 nT, as shown in Figure 1f, imply that a moderate storm take placed' in the line 61-62.

There is no space between words in many places throughout the text. Put space between the words throughout the text.

Responses: Thank you for this comment. We have checked space between the words throughout the text.

Interactive comment on “Magnetic dipolarizations inside geosynchronous orbit with tailward ions flow” by Xiaoying Sun et al.

Anna Milillo (Editor)
anna.milillo@inaf.it
Received and published: 6 February 2019

Comments: This paper reports the observations of two dipolarizations linked to a substorm registered by the two THEMIS spacecraft E and D located one inside the geosynchronous orbit and the other tailward. The paper is well written. Essentially I agree with the other referee that some more check should be done to prove the double dipolarization occurrence. Also there is some confusion with the Electric field directions and flow velocity directions. I will recommend it for publication after these revisions.

Responses: We thank you for your comments that help improving the manuscript. In light of your comments, we have revised the manuscript accordingly.

Comments: Minor comments line 33 NESP should be NEPS line 69: the z coordinates of the two s/c here are probably wrong, since both are in the plasma sheet, in fact in the figures 3 and 4 there are different values. there are many typos and missing spaces within the manuscript.

Responses: Thank you for these comments. According to your suggestion we have revised the spacecraft orbit data shown in line 69-70 as ‘locations of these two spacecraft in SM coordinates, are (-6.10, -0.06, 0.43) R_E for TH-D, (-8.26, -2.28, 0.99) R_E for TH-E, respectively’. During this intense geomagnetic activity, the magnetic equator plane tilt towards southward, the small Z coordinate of TH-E does not mean it is located in the plasma sheet based on the plasma density, temperature and beta value as in Figure 4 in our paper.
We have checked space between the words throughout the text.

A list of all relevant changes made in the manuscript

Line 33-35 (revised): 'Especially, it is more complex in the inner edge of ~~NESP~~ NEPS. Usually, the substorm-associated dipolarizations in the NEPS are accompanied with earthward ions bulk flow [e.g., Angelopoulos et al., 1992; Baumjohann et al., 1999; Duan et al., 2011; Liang et al., ~~2008~~ 2009; Liu et al., 2008 …'

Line 42 (deleted): 'Liang et al., ~~2008,~~ 2009;'

Line 56 (revised): 'In this paper we present ~~a~~ dipolarizations with tailward ions flow inside geosynchronous orbit…'

Line 61-63 (revised): 'The minimum value of ~~Dst~~ SYM-H index is about ~~-80~~ -90 nT, as shown in Figure ~~1e~~ 1f, imply that a moderate storm take placed. During the main phase of this moderate storm, there is an intense substorm with the AE maximum value ~~1273~~ 700 nT around 10:10 UT.'

Line 69-70 (revised): '…locations of these two spacecraft in SM coordinates, are (~~-6.01~~ -6.10, -0.06, ~~1.12~~ 0.43) R_E for TH-D, (~~-8.10~~ -8.26, -2.28, ~~1.92~~ 0.99) R_E for TH-E, respectively.'

Line 91-92(revised): '…The electron density and temperature both increase. The ion density also increases. But ion temperature decreases. Accompanied this…'

Line 149-158 (added): 'consistent with each other. The dipolarization associated with the current disruption propagated tailward with speed V_x ~ -100 km/s detected by THEMIS satellites in the near-Earth plasma sheet X ~ -11R_E [Liu et al., 2008]. It is larger than the dipolarization propagating speed from inside to outside geosynchronous orbit V_x ~ -47 km/s . The different speeds of dipolarizations propagating tailward imply that the magnitude of the dipolarization speed may be associated with its beginning location in magnetotail plasma sheet.

On the other hand, Lui [1991] reported that substorm disturbance propagated tailward through a rarefaction wave front accompanied by earthward flow during substorm expansion phase early period. Chao et al. [1977] proposed that the rarefaction wave propagating tailward was accompanied by the thinning of plasma sheet and earthward plasma flow. This earthward flow is possibly convection flow or outflow flow of magnetic reconnection from the middle magnetotail.'

Line 193-194 (added): 'Chao J., K ., J. R . Kan, A . T. Y. Lui and S .-I. Akasofu A model for thinning of the plasma sheet, Planet. Space Sci., 25, 703-710, 1977.'

Line 214-216 (deleted): '~~Liang, J., Donovan, E. F., Liu, W. W., Jackel, B., Syrjäsuo, M., Mende, S. B., Frey, H. U., Angelopoulos, V., and Connors, M.: Intensification of preexisting auroral arc at substorm expansion phase onset: Wave-like disruption during the first tens of seconds, Geophysical Research Letters, 35, 2008.~~'

Line 233 (added): 'Lui, A. T. Y., A synthesis of magnetospheric substorm models, Journal of Geophysical Research, 96,1849, 1991.'

A marked-up manuscript version

Magnetic dipolarizations inside geosynchronous orbit with tailward ions flow

Xiaoying Sun[1,2], Weining William Liu [1], Suping Duan[1]

[1] State Key Laboratory of Space Weather, National Space Science Center (NSSC),Chinese Academy of Sciences (CAS), Beijing, 100190, China
[2]University of Chinese Academy of Sciences, Beijing, 100049, China

Correspondence to: W .W. Liu (wliu@nssc.ac.cn), Suping Duan (spduan@nssc.ac.cn)

Abstract. Electromagnetic field and plasma data from the Time History of Events and Macroscale Interactions during Substorms (THEMIS) near-Earth probes are used to investigate magnetic dipolarizations inside geosynchronous orbit on 27 August 2014 during an intense substorm with AE_{max} ~ 1000nT. THEMIS-D (TH-D) was located inside geosynchronous orbit around midnight in the interval from 09:25 UT to 09:55 UT. During this period two distinct magnetic dipolarizations with tailward ions flow are observed by TH-D. The first one is displayed by magnetic elevation angle increase from 15 degree to 25 degree around 09:30:40UT. The tailward perpendicular velocity is $V_{\perp x}$ ~ -50km/s. The second one is presented by the elevation angle increase from 25 degree to 45 degree around 09:36 UT. And the tailward perpendicular velocity is $V_{\perp x}$ ~ -70 km/s. These two significant dipolarizations are accompanied with the sharp increase in the energy flux of energetic electron inside geosynchronous. After 5 min expanding of near-Earth plasma sheet (NEPS), THEMIS-E (TH-E) located outside geosynchronous orbit also detects this tailward expanding plasma sheet with ion flow -150 km/s. The dipolarization propagates tailward with speed -47 km/s, along 2.2 R_E distance in the X direction between TH-D and TH-E within 5 min. These dipolarizations with tailward ions flow observed inside geosynchronous orbit indicate new energy transfer path in the inner magnetosphere during substorms.

Keywords: Magnetic dipolarization, tailward ions flow, near-Earth plasma sheet, intense substorm

Introduction

Magnetic dipolarization can be observed at or inside geosynchronous orbit during intense substorms with high AE index (AE > 500 nT) [e.g., Dai et al., 2015; Nagai, 1982; Nosé et al., 2014; Ohtani et al., 2018]. Dipolarizations are marked by the magnetic elevation angle increase with the decrease in the radial components of B_x and B_y, and the increase in the B_z component [Liu and Liang, 2009; Duan et al., 2011; Dai et al., 2014, 2015]. Ohtani et al. [2018] presented the statistics characteristics of magnetic dipolarizations inside geosynchronous orbit. They reported that the dipolarization region expanded in the azimuthal direction with speed 60 km/s at 5.5 R_E. Using multiple satellites conjunction observations at or inside geosynchronous orbit, Dai et al. [2015] reported that the large dipolarization electric field was associated with substorm injection of MeV electrons into the inner magnetosphere (r < 6.6 R_E).

Magnetic dipolarizations are accompanied with complex ions bulk flow in the near-Earth plasma sheet (NEPS) [e.g., Duan et al., 2008; Liang et al., 2009]. Especially, it is more complex in the inner edge of ~~NESP~~ NEPS. Usually, the substorm-associated dipolarizations in the NEPS are accompanied with earthward ions bulk flow [e.g., Angelopoulos et al., 1992; Baumjohann et al., 1999; Duan et al., 2011; Liang et al., ~~2008~~ 2009; Liu et al., 2008; Nakamura et al., 2009; Shiokawa et al., 1998]. According conjunction observations of THEMIS multiple probes in the NEPS, Duan et al. [2011] pointed out that the dipolarization at inner edge of the near-Earth plasma sheet had no one-to-one relationship with the earthward ions bulk flow. Lui et al. [1999] pointed out that dipolarization at $X{\sim}10R_E$ was detected with tailward flow. Inside geosynchronous orbit, magnetic dipolarizations were detected with earthward ions bulk flow [Dai et al., 2015].

Near-Earth Dipolarizations with low frequency waves are detected with thermal ions and electron energization [e.g., Dai et al., 2015; Liang et al., ~~2008,~~ 2009; Nosé et al., 2014; Ohtani et al., 2018]. These energetic particles are main source of inner magnetosphere during substorms and storms. Nosé et al. [2014] proposed that the dipolarizations associated with low frequency fluctuations were observed in the inner magnetosphere during the storm main phase. These low frequency electromagnetic waves can accelerate O^+ ions in the perpendicular direction. The low frequency waves can accelerate particles crossing the magnetic field with large perpendicular electric field [e.g., Dai et al., 2014, 2015; Duan et al., 2016; Nosé et al., 2014]. Usually, Dipolarization associated dispersionless energetic particle injections is accompanied with earthward ions bulk flow in the NEPS [Dai et al., 2015]. But few reports show that dipolarizations with the sharply increase in the energy flux of energetic particles associated with tailward ions flow at or inside geosynchronous orbit.

The ballooning mode occurred in the near-Earth plasma sheet are associated with tailward expansion of plasma sheet during substorms [Liu, 1997; Liu et al., 2008; Liu and Liang, 2009; Liang et al., 2009; Saito et al., 2008]. Liu et al. [2008] pointed out that the ballooning mode could excite a quasi-electrostatic field a few minutes before local current disruption and that the perturbations associated with ballooning instability propagated downtail.

In this paper we present ~~a~~ dipolarizations with tailward ions flow inside geosynchronous orbit during an intense substorm expansion phase. The observations in detail of an intense substorm on 27 August 2014 by TH-D and TH-E are presented in section 2. Discussions and conclusions of our observation results are displayed in the last section.

Observations of an intense substorm on 27 August 2014

The OMNI data of the solar wind, interplanetary magnetic field (IMF) and geomagnetic field index Dst and AE during a storm on August 27, 2014 are presented in Figure 1. The minimum value of ~~Dst~~ SYM-H index is about ~~-80~~ -90 nT, as shown in Figure ~~1e~~ 1f, imply that a moderate storm take placed. During the main phase of this moderate storm, there is an intense substorm with the AE maximum value ~~1273~~ 700 nT around 10:10 UT. The beginning time of this intense substorm expansion phase is around 09:31 UT with decrease in the AL index. A significant substorm enhancement occur around 09:48 UT with sharply decrease in the AL index and increase in the AE index.

During this intense substorm, THEMIS probes [Angelopoulos, 2008], such as TH-D and TH-E are both located in the near-Earth magnetotail. Figure 2 displays the orbits of TH-D and TH-E from 09:20 to 10:00 UT in the SM coordinate system. At 09:30 UT, locations of these two spacecraft in SM coordinates, are (~~-6.01~~ -6.10, -0.06, ~~1.12~~ 0.43) R_E for TH-D, (~~-8.10~~ -8.26, -2.28, ~~1.92~~ 0.99) R_E for TH-E, respectively. TH-D orbit plot presents that it is located inside geosynchronous orbit at the beginning time of this intense substorm expansion phase. On the other hand, TH-E is located outside geosynchronous orbit. These two spacecraft present good conjunction observations during this intense substorm expansion phase. The instruments adopted in our investigations are the fluxgate magnetometer (FGM) [Auster et al., 2008], the electrostatic analyzer (ESA) [McFadden et al., 2008], the electric field instrument (EFI) [Bonnell et al., 2008] and the solid state telescope (SST) on board the THEMIS probes.

Figure 3 shows the plasma parameters and the electromagnetic field detected by TH-D mostly inside geosynchronous orbit at about midnight section. The solar magnetic (SM) coordinate system is adopted. From top to bottom, panels are the total magnetic field value, B_t and the B_x component, the B_y and B_z components, the magnetic field elevation angle defined by $\theta = \tan^{-1}(B_z/({B_x}^2 + {B_y}^2)^{1/2})$, the ion and electron density, temperature, the plasma beta value β, $\beta = 2\mu_0 nT/B^2$, which determines the location of the satellite [Miyashita et al., 2000], three components of ions bulk flow velocity parallel (black line) and perpendicular (red line) to the magnetic field, V_x, V_y and V_z, three components of the electric field, the E_x (red), the E_y (black) and the E_z (blue), there components of convection electric field from **V**×**B**, the E_{cx} (red), the E_{cy} (black) and the E_{cz}(blue), respectively. Figure 3 displays the distinct fluctuations of the magnetic field and plasma density and velocity around 09:30 UT and 09:36 UT, respectively. The magnetic elevation angle has two step clear enhancements as displayed in Figure 3c. The first increase in elevation angle is from about 15 degree to 25 degree during the interval from 09:30:34 UT to 09:30:54 UT, which are marked by the left two vertical dashed lines in Figure 3. The total magnetic field value and the B_x component both decrease. The B_z component increase weakly from about 35 nT to 45 nT. The B_y component has obvious fluctuations around 0 nT. These magnetic signatures indicate a magnetic dipolarization take places inside geosynchronous orbit around (-6.10, -0.06, 0.43) R_E. During this weak magnetic field dipolarization, the plasma beta value, β, increases from around 0.5 to 1.0. The electron density and temperature both increase. The ion density also increases. But ion temperature decreases. Accompanied this dipolarization the tailward ions bulk flow, $V_{//x}$ ~ -100km/s and the perpendicular component to the magnetic field in the X direction, $V_{\perp x}$ ~ -50 km/s is detected by TH-D, as shown in Figure 3g. The perpendicular velocity in the Y direction is mainly dawnward at the beginning time of this dipolarization, $V_{\perp y}$ ~ -30km/s. The electric field detected by TH-D also has large fluctuations with negative E_y value during the first depolarization as shown in Figure 3j. During the intervals from 09:30:34 UT to 09:30:54 UT the convection electric field direction is dawnward with large magnitude, E_{cy} ~ -12 mV/m, as presented in Figure 3k. The second magnetic field elevation angle increases sharply at around 09:36 as displayed in Figure 3c marked by the right two vertical dashed lines. The elevation angle increases from about 25 degree to 45 degree during the interval from 09:36:06 UT to 09:36:21UT. The magnetic field has similar variations to the first dipolarization signatures. Especially, the second dipolarization has larger elevation angle maximum value, ~ 45 degree, as marked by the fourth vertical dashed line in Figure 3c. During the second dipolarization the tailward ions bulk flow perpendicular to the magnetic field is also detected by TH-D, $V_{\perp x}$ ~ -70 km/s, as presented in Figure 3g. Also the significant negative E_y component is companied by this intense dipolarization in Figure 3j and 3k.

During the intervals of magnetic dipolarizations with tailward ions bulk flow detected by TH-D inside geosynchronous orbit, TH-E observed very weak increase in the magnetic field elevation angle and the B_z component around 09:35 UT and 09:41 UT, as shown in Figure 4b and 4c, about 5 min after two dipolarizations detected by TH-D. The ions and electron density and temperature increase weakly from very low value as displayed in Figure 4d and 4e. Outside geosynchronous orbit, TH-E observed very low beta value, as shown in Figure 4f, β ~ 0.01 and β ~ 0.2 around 09:35 UT and 09:41 UT, respectively. Interesting phenomena that the weak dipolarization was with the tailward ions bulk flow, $V_{//x}$ ~ -180km/s, is also detected by TH-E around 09:35 UT as shown in Figure 4g. The perpendicular velocity is dominated in the negative Y direction, $V_{\perp y}$ ~ -50 km/s.

Associated with the intense electric field observed by TH-D inside geosynchronous orbit during this two dipolarizations, the energy fluxes of energetic electrons, as shown in the second panel of Figure 5, with energy of 31 keV(blue), 41 keV (gray), 52 keV (red), 65.5 keV (black), 93 keV(brown) and 139 keV(purple) all simultaneously increase at 09:30:38 UT and 09:36:09UT detected by SST/TH-D, respectively. These energetic electrons have quasi-perpendicular pitch angle distribution, as presented in the bottom panel of Figure 5.

Discussion and conclusions

The dipolarizations with tailward ions bulk flow inside geosynchronous orbit are investigated in our present paper. Accompanied these dipolarizations the energy fluxes of energetic electrons with energy between 31 keV and 139 keV simultaneously increase inside geosynchronous orbit. According to these energetic electrons pitch angle distributions, it is found that high energy electrons mainly in the quasi-perpendicular direction to the magnetic field, as shown in Figure 5. On the other hand, the inductive electric field during these two magnetic dipolarization is in the dawnward direction as display in Figure 3j and 3k. Previous research work reported that the inductive electric field associated with substorm dipolarization can accelerate particles in the near-Earth plasma sheet [e.g. Dai et al., 2014, 2015; Duan et al., 2016; Fu et al., 2011; Fok et al., 2001; Liu et al., 2010; Lui et al., 1988, 1999; Nakamura et al., 2009; Nosé et al., 2014]. As shown in Figure 3j around 09:36:30 UT the inductive electric fields in the second dipolarization are dominated in the E_y component with large negative value, E_y ~ -25mV/m, and the X component also increase with negative value E_x ~ -6mV/m. This intense electric field can drive ions moving into the tailward-dawnward direction. On the other hand, we can calculate the energy quantity relationship between the electric field and energetic electrons. Estimating the energy of such intense E_y in the distance of ~1000 km is about ~ 10^{-15} Joule. The energetic electrons with energy range from 31 keV to 139 keV are in the same energy order ~10^{-15} Joule. It is inferred that the intense E_y can perpendicularly accelerate electrons to tens keV state.

Dipolarizations occurring at the inner edge of plasma sheet are complicated with disturbances of ions bulk flow and electromagnetic field. Lui et al. [1999] pointed out that near-Earth dipolarization was a non-MHD process and was also accompanied with tailward ions flow. Our observations of dipolarizations inside geosynchronous orbit are also associated with tailward ions flow. This result is consistent with the report proposed by Liu et al. [2008] that the perturbations associated with the ballooning mode in the near-Earth plasma sheet propagating tailward. Based on the statistic studies, Nosé et al. [2016] proposed that the occurrence probability of the dipolarizations in the inner magnetosphere had a peak at 21:00-00:00 MLT. Our observations show that two distinct dipolarizations with tailward flow inside geosynchronous orbit are detected by TH-D around 00:02 MLT and 00:05 MLT, respectively.

According to the distance between TH-D and TH-E, (-2.23, -2.30, 0.56)R_E, and the delay time of dipolarization from inside to outside geosynchronous orbit, ~5 min, the dipolarization propagating speed or the plasma sheet expanding speed can be estimated as V_x ~ -47 km/s, V_y ~ -48 km/s, V_z ~ 12 km/s, respectively. Liou et al. [2002] proposed that the dipolarization region expanding speed was ~ 60 km/s westward at geosynchronous. Comparing observations between TH-D and TH-E in our investigations, the azimuth speed of dipolarization region is obtained ~ 48 km/s. These two observational results are consistent with each other. The dipolarization associated with the current disruption propagated tailward with speed V_x ~ -100 km/s detected by THEMIS satellites in the near-Earth plasma sheet X ~ -11R_E [Liu et al., 2008]. It is larger than the dipolarization propagating speed from inside to outside geosynchronous orbit V_x ~ -47 km/s. The different speeds of dipolarizations propagating tailward imply that the magnitude of the dipolarization speed may be associated with its beginning location in magnetotail plasma sheet.

On the other hand, Lui [1991] reported that substorm disturbance propagated tailward through a rarefaction wave front accompanied by earthward flow during substorm expansion phase early period. Chao et al. [1977] proposed that the rarefaction wave propagating tailward was accompanied by the thinning of plasma sheet and earthward plasma flow. This earthward flow is possibly convection flow or outflow flow of magnetic reconnection from the middle magnetotail.

Based on the above observation analysis, we can draw the results as following. Two distinct magnetic dipolarizations with tailward ions flow are observed by TH-D inside geosynchronous orbit on 27 August 2014 during the intense substorm with AE_{max} ~ 1000nT. TH-D was located inside geosynchronous orbit around midnight in the interval from 09:20 UT to 10:00 UT. The first dipolarization is displayed by magnetic elevation angle increase from 15 degree to 25 degree around 09:30:40UT. The second one is presented by the elevation angle increase from 25 degree to 45 degree around 09:36 UT. These two significant dipolarizations are accompanied with the energy flux of energetic electrons simultaneously increase inside geosynchronous orbit. After 5 min expanding tailward of near-Earth plasma sheet, TH-E located outside geosynchronous orbit also detects this tailward expanding plasma sheet with ion flow -150 km/s. The dipolarization propagates tailward with speed -45 km/s, along 2 R_E distant in the X direction between TH-D and TH-E within 5 min. These dipolarizations with tailward ion flow observed inside geosynchronous orbit indicate new energy transfer path in the inner magnetosphere during substorms.

Acknowledgments

We acknowledge NASA contract NAS5-02099 for use of data from the THEMIS Mission. Specifically: “D. Larson and R. P. Lin for use of SST data, C. W. Carlson and J. P. McFadden for use of ESA data; J. Bonnell and F. S. Mozer for use of the EFI data; K. H. Glassmeier, U. Auster and W. Baumjohann for the use of FGM data provided under the lead of the Technical University of Braunschweig and with financial support through the German Ministry for Economy and Technology and the German Center for Aviation and Space (DLR) under contract 50 OC 0302. The authors thank NASA CDAWeb and Taiwan AIDA for THEMIS data. The $\mathrm{SYM-H}$ index was provided by Data Analysis Center for Geomagnetism and Space Magnetism in Kyoto, Japan. This work is supported by the National Natural Science Foundation of China grants 41674167, 41731070 and 41574161; and in part by the Specialized Research Fund for State Key Laboratories.

References

Angelopoulos, V.: The THEMIS Mission, Space Science Reviews, 141, 5-34, 2008.

Angelopoulos, V., Baumjohann, W., Kennel, C. F., Coroniti, F. V., Kivelson, M. G., Pellat, R., Walker, R. J., Lühr, H., and Paschmann, G.: Bursty bulk flows in the inner central plasma sheet, Journal of Geophysical Research, 97, 4027, 1992.

Auster, H. U., Glassmeier, K. H., Magnes, W., Aydogar, O., Baumjohann, W., Constantinescu, D., Fischer, D., Fornacon, K. H., Georgescu, E., Harvey, P., Hillenmaier, O., Kroth, R., Ludlam, M., Narita, Y., Nakamura, R., Okrafka, K., Plaschke, F., Richter, I., Schwarzl, H., Stoll, B., Valavanoglou, A., and Wiedemann, M.: The THEMIS Fluxgate Magnetometer, Space Science Reviews, 141, 235-264, 2008.

Baumjohann, W., Hesse, M., Kokubun, S., Mukai, T., Nagai, T., and Petrukovich, A. A.: Substorm dipolarization and recovery, Journal of Geophysical Research: Space Physics, 104, 24995-25000, 1999.

Bonnell, J. W., Mozer, F. S., Delory, G. T., Hull, A. J., Ergun, R. E., Cully, C. M., Angelopoulos, V., and Harvey, P. R.: The Electric Field Instrument (EFI) for THEMIS, Space Science Reviews, 141, 303-341, 2008.

Chao J., K ., J. R . Kan, A . T. Y. Lui and S .-I. Akasofu A model for thinning of the plasma sheet, Planet. Space Sci., 25, 703-710, 1977.

Dai, L., Wang, C., Duan, S., He, Z., Wygant, J. R., Cattell, C. A., Tao, X., Su, Z., Kletzing, C., Baker, D. N., Li, X., Malaspina, D., Blake, J. B., Fennell, J., Claudepierre, S., Turner, D. L., Reeves, G. D., Funsten, H. O., Spence, H. E., Angelopoulos, V., Fruehauff, D., Chen, L., Thaller, S., Breneman, A., and Tang, X.: Near-Earth injection of MeV electrons associated with intense dipolarization electric fields: Van Allen Probes observations, Geophys Res Lett, 42, 6170-6179, 2015.

Dai, L., Wygant, J. R., Cattell, C. A., Thaller, S., Kersten, K., Breneman, A., Tang, X., Friedel, R. H., Claudepierre, S. G., and Tao, X.: Evidence for injection of relativistic electrons into the Earth's outer radiation belt via intense substorm electric fields, Geophysical Research Letters, 41, 1133-1141, 2014.

Duan, S., Liu, Z., Cao, J., Lu, L., Rème, H., Dandouras, I., and Carr, C. M.: TC-1 observation of ion high-speed flow reversal in the near-Earth plasma sheet during substorm, Science in China Series E: Technological Sciences, 51, 1721-1730, 2008.

Duan, S. P., Dai, L., Wang, C., Liang, J., Lui, A. T. Y., Chen, L. J., He, Z. H., Zhang, Y. C., and Angelopoulos, V.: Evidence of kinetic Alfven eigenmode in the near-Earth magnetotail during substorm expansion phase, Journal of Geophysical Research-Space Physics, 121, 4316-4330, 2016.

Duan, S. P., Liu, Z. X., Liang, J., Zhang, Y. C., and Chen, T.: Multiple magnetic dipolarizations observed by THEMIS during a substorm, Annales Geophysicae, 29, 331-339, 2011.

Fok, M.-C., Moore, T. E., and Spjeldvik, W. N.: Rapid enhancement of radiation belt electron fluxes due to substorm dipolarization of the geomagnetic field, Journal of Geophysical Research: Space Physics, 106, 3873-3881, 2001.

Fu, H. S., Khotyaintsev, Y. V., André, M., and Vaivads, A.: Fermi and betatron acceleration of suprathermal electrons behind dipolarization fronts, Geophysical Research Letters, 38, n/a-n/a, 2011.

~~Liang, J., Donovan, E. F., Liu, W. W., Jackel, B., Syrjäsuo, M., Mende, S. B., Frey, H. U., Angelopoulos, V., and Connors, M.: Intensification of preexisting auroral arc at substorm expansion phase onset: Wave-like disruption during the first tens of seconds, Geophysical Research Letters, 35, 2008.~~

Liang, J., Liu, W. W., and Donovan, E. F.: Ion temperature drop and quasi-electrostatic electric field at the current sheet boundary minutes prior to the local current disruption, Journal of Geophysical Research: Space Physics, 114, n/a-n/a, 2009.

Liou, K., Meng, C.-I., Lui, A. T. Y., Newell, P. T., and Wing, S.: Magnetic dipolarization with substorm expansion onset, Journal of Geophysical Research, 107, 2002.

Liu, W. W.: Physics of the explosive growth phase: Ballooning instability revisited, Journal of Geophysical Research: Space Physics, 102, 4927-4931, 1997.

Liu, W. W. and Liang, J.: Disruption of magnetospheric current sheet by quasi-electrostatic field in the substorm expansion phase, Annales Geophysicae, 27, 1941-1950, 2009.

Liu, W. W., Liang, J., and Donovan, E. F.: Electrostatic field and ion temperature drop in thin current sheets: A theory, Journal of Geophysical Research: Space Physics, 115, n/a-n/a, 2010.

Liu, W. W., Liang, J., and Donovan, E. F.: Interaction between kinetic ballooning perturbation and thin current sheet: Quasi-electrostatic field, local onset, and global characteristics, Geophysical Research Letters, 35, 2008.

Lui, A. T. Y., Liou, K., Nosé, M., Ohtani, S., Williams, D. J., Mukai, T., Tsuruda, K., and Kokubun, S.: Near-Earth dipolarization: Evidence for a non-MHD process, Geophysical Research Letters, 26, 2905-2908, 1999.

Lui, A. T. Y., Lopez, R. E., Krimigis, S. M., McEntire, R. W., Zanetti, L. J., and Potemra, T. A.: A case study of magnetotail current sheet disruption and diversion, Geophysical Research Letters, 15, 721-724, 1988.

Lui, A. T. Y., A synthesis of magnetospheric substorm models, Journal of Geophysical Research, 96,1849, 1991.

McFadden, J. P., Carlson, C. W., Larson, D., Ludlam, M., Abiad, R., Elliott, B., Turin, P., Marckwordt, M., and Angelopoulos, V.: The THEMIS ESA Plasma Instrument and In-flight Calibration, Space Science Reviews, 141, 277-302, 2008.

Miyashita, Y., Machida, S., Mukai, T., Saito, Y., Tsuruda, K., Hayakawa, H., and Sutcliffe, P. R.: A statistical study of variations in the near and middistant magnetotail associated with substorm onsets: GEOTAIL observations, Journal of Geophysical Research: Space Physics, 105, 15913-15930, 2000.

Nagai, T.: Observed magnetic substorm signatures at synchronous altitude, Journal of Geophysical Research, 87, 4405, 1982.

Nakamura, R., Retino, A., Baumjohann, W., Volwerk, M., Erkaev, N., Klecker, B., Lucek, E. A., Dandouras, I., Andre, M., and Khotyaintsev, Y.: Evolution of dipolarization in the near-Earth current sheet induced by Earthward rapid flux transport, Annales Geophysicae, 27, 1743-1754, 2009.

Nosé, M., Keika, K., Kletzing, C. A., Spence, H. E., Smith, C. W., MacDowall, R. J., Reeves, G. D., Larsen, B. A., and Mitchell, D. G.: Van Allen Probes observations of magnetic field dipolarization and its associated O+ flux variations in the inner magnetosphere at L < 6.6, Journal of Geophysical Research-Space Physics, 121, 7572-7589, 2016.

Nosé, M., Takahashi, K., Keika, K., Kistler, L. M., Koga, K., Koshiishi, H., Matsumoto, H., Shoji, M., Miyashita, Y., and Nomura, R.: Magnetic fluctuations embedded in dipolarization inside geosynchronous orbit and their associated selective acceleration of O+ ions, Journal of Geophysical Research: Space Physics, 119, 4639-4655, 2014.

Ohtani, S., Motoba, T., Gkioulidou, M., Takahashi, K., and Singer, H. J.: Spatial Development of the Dipolarization Region in the Inner Magnetosphere, Journal of Geophysical Research: Space Physics, 123, 5452-5463, 2018.

Saito, M. H., Miyashita, Y., Fujimoto, M., Shinohara, I., Saito, Y., Liou, K., and Mukai, T.: Ballooning mode waves prior to substorm-associated dipolarizations: Geotail observations, Geophysical Research Letters, 35, n/a-n/a, 2008.

Shiokawa, K., Baumjohann, W., Haerendel, G., Paschmann, G., Fennell, J. F., Friis-Christensen, E., Lühr, H., Reeves, G. D., Russell, C. T., Sutcliffe, P. R., and Takahashi, K.: High-speed ion flow, substorm current wedge, and multiple Pi 2 pulsations, Journal of Geophysical Research: Space Physics, 103, 4491-4507, 1998.

Copernicus Publications
The Innovative Open Access Publisher

Figure 1 The solar wind, IMF $\boldsymbol{B_z}$ conditions and geomagnetic indices between 01:00 UT and 23:00 UT on August 27, 2014. From top to bottom of (a ~ g) panels show the change of solar wind dynamic pressure (a), $\boldsymbol{B_{z,IMF}}$ in GSM coordinate (b), the x component of the solar wind flow speedin GSM coordinate (c), electric field$\boldsymbol{E}$ (d), *AE/AU/AL* index (e),*SYM-H* indices (f), and *ASY-H* index (g). From left to right, the verticaldotted lines in (a ~ g) panels marked the time 01:48 UT, 06:42 UT, 09:31 UT, 09:48 UT, 21:56 UT and 22:35 UT, respectively.

Figure 2 The orbits of TH-D and TH-E in the $\boldsymbol{X - Y_{SM}}$ plane and the $\boldsymbol{X - Z_{SM}}$ plane from 09:20 to 10:00 UT on 27 August 2014, which were in the nightside magnetosphere. The arrow shows the flying direction of the satellites. TH-D is redand TH-E is blue.

Figure 3 The electromagnetic field and plasma parameters detected by TH-D in the intervals from 09:25 UT to 09:55 UT on August 27, 2014. The Solar Magnetic (SM) coordinated system is adopted. From top to bottom, panels showed that (a)the total magnetic field $\boldsymbol{B_t}$ (black) and the X component $\boldsymbol{B_x}$ (red), (b) the Y component $\boldsymbol{B_y}$ (green) and the Z component $\boldsymbol{B_z}$ (blue), (c)the magnetic field elevation angle $\boldsymbol{\theta}$; (d) ion and electron density $\boldsymbol{N_i}$, $\boldsymbol{N_e}$; (e)ion and electron temperature $\boldsymbol{T_i}$, $\boldsymbol{T_e}$; (f) plasma beta $\boldsymbol{\beta}$; (g) the X component of ion parallelvelocity and perpendicular velocity$\boldsymbol{V_{parx}}$, $\boldsymbol{V_{perpx}}$; (h) the Y component of ion parallel velocity and perpendicularvelocity $\boldsymbol{V_{pary}}$,$\boldsymbol{V_{perpy}}$; (i) the Z component of ion parallel velocity and perpendicular velocity $\boldsymbol{V_{parz}}$, $\boldsymbol{V_{perpz}}$; (j) the electric field $\boldsymbol{E_x}$ (red), $\boldsymbol{E_y}$ (black), and $\boldsymbol{E_z}$ (blue) by assuming $\mathbf{E} \cdot \mathbf{B} = \mathbf{0}$; (k) the electric field $\boldsymbol{E_{cx}}$ (red), $\boldsymbol{E_{cy}}$ (black), $\boldsymbol{E_{cz}}$ (blue) calculated by $\mathbf{E} = \mathbf{B} \times \mathbf{V}$. The black vertical dashed lines marked the time 09:30:34 UT, 09:30:54UT, 09:36:06 UT and 09:36:21 UT, respectively.

Figure 4 The electromagnetic field and plasma parameters detected by TH-E in the intervals from 09:25 UT to 09:55 UT on August 27, 2014.The Figure format is the same as Figure 3.The black vertical dashed lines marked the time 09:35:36 UT and 09:36:18 UT.

Figure 5 The energy flux and pitch angle distribution of energetic electrons detected by SST/TH-D in 3 second time resolution. The red vertical lines marked the time 09:30:38 UT and 09:36:09 UT.

Figure 1

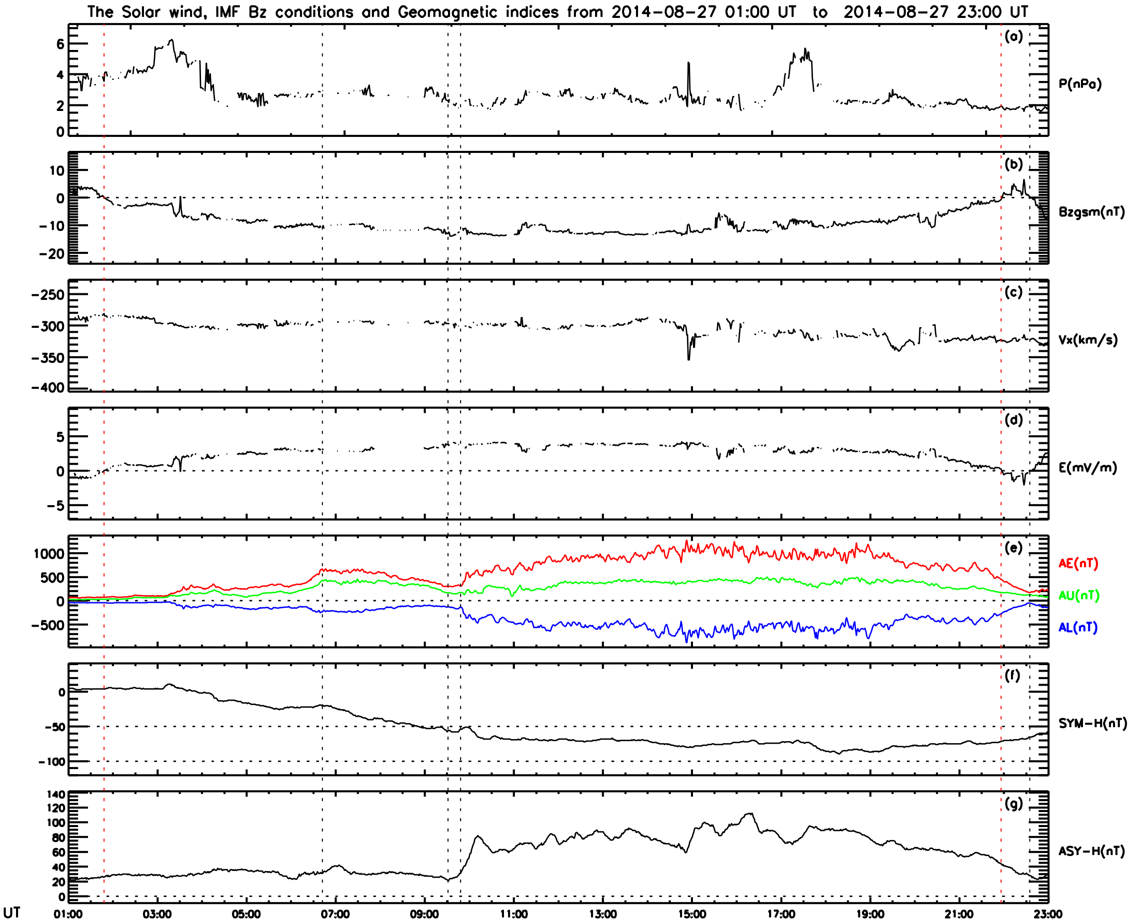

Figure 2

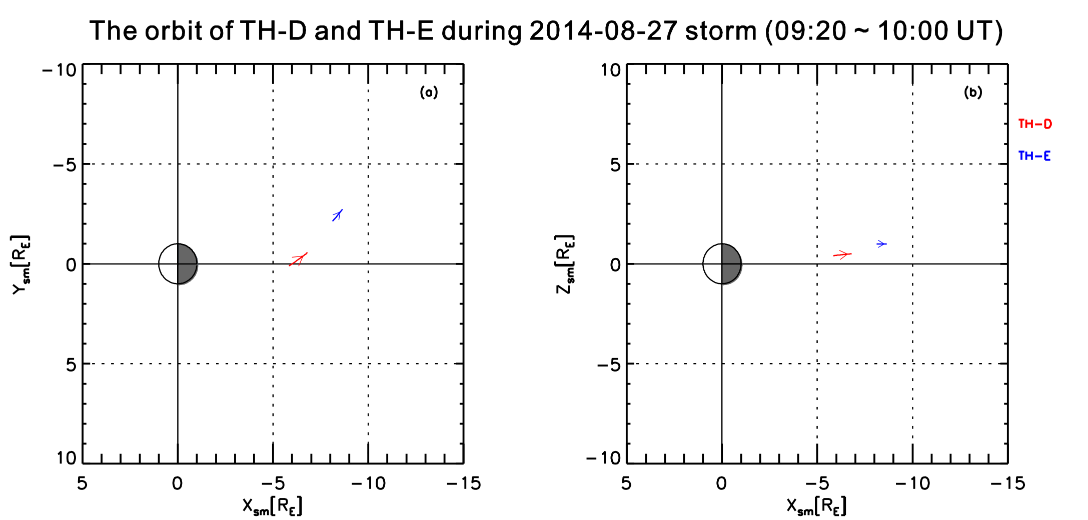

Figure 3

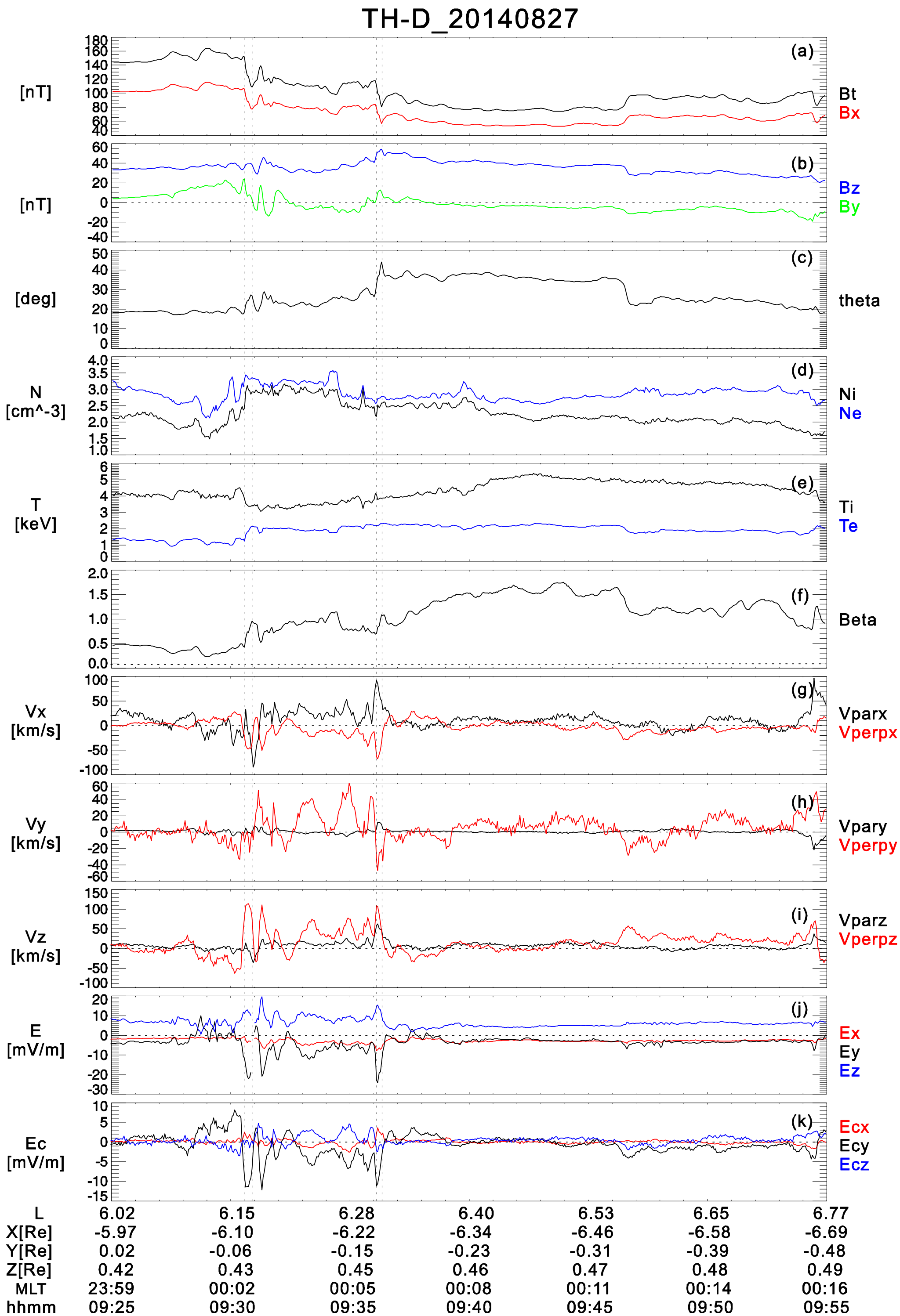
TH-D_20140827
(a)
[nT]
Bt
Bx
(b)
[nT]
Bz
By
(c)
[deg]
theta
(d)
N [cm^-3]
Ni
Ne
(e)
T [keV]
Ti
Te
(f)
Beta
(g)
Vx [km/s]
Vparx
Vperpx
(h)
Vy [km/s]
Vpary
Vperpy
(i)
Vz [km/s]
Vparz
Vperpz
(j)
E [mV/m]
Ex
Ey
Ez
(k)
Ec [mV/m]
Ecx
Ecy
Ecz
L 6.02 6.15 6.28 6.40 6.53 6.65 6.77
X[Re] -5.97 -6.10 -6.22 -6.34 -6.46 -6.58 -6.69
Y[Re] 0.02 -0.06 -0.15 -0.23 -0.31 -0.39 -0.48
Z[Re] 0.42 0.43 0.45 0.46 0.47 0.48 0.49
MLT 23:59 00:02 00:05 00:08 00:11 00:14 00:16
hhmm 09:25 09:30 09:35 09:40 09:45 09:50 09:55

Figure 4

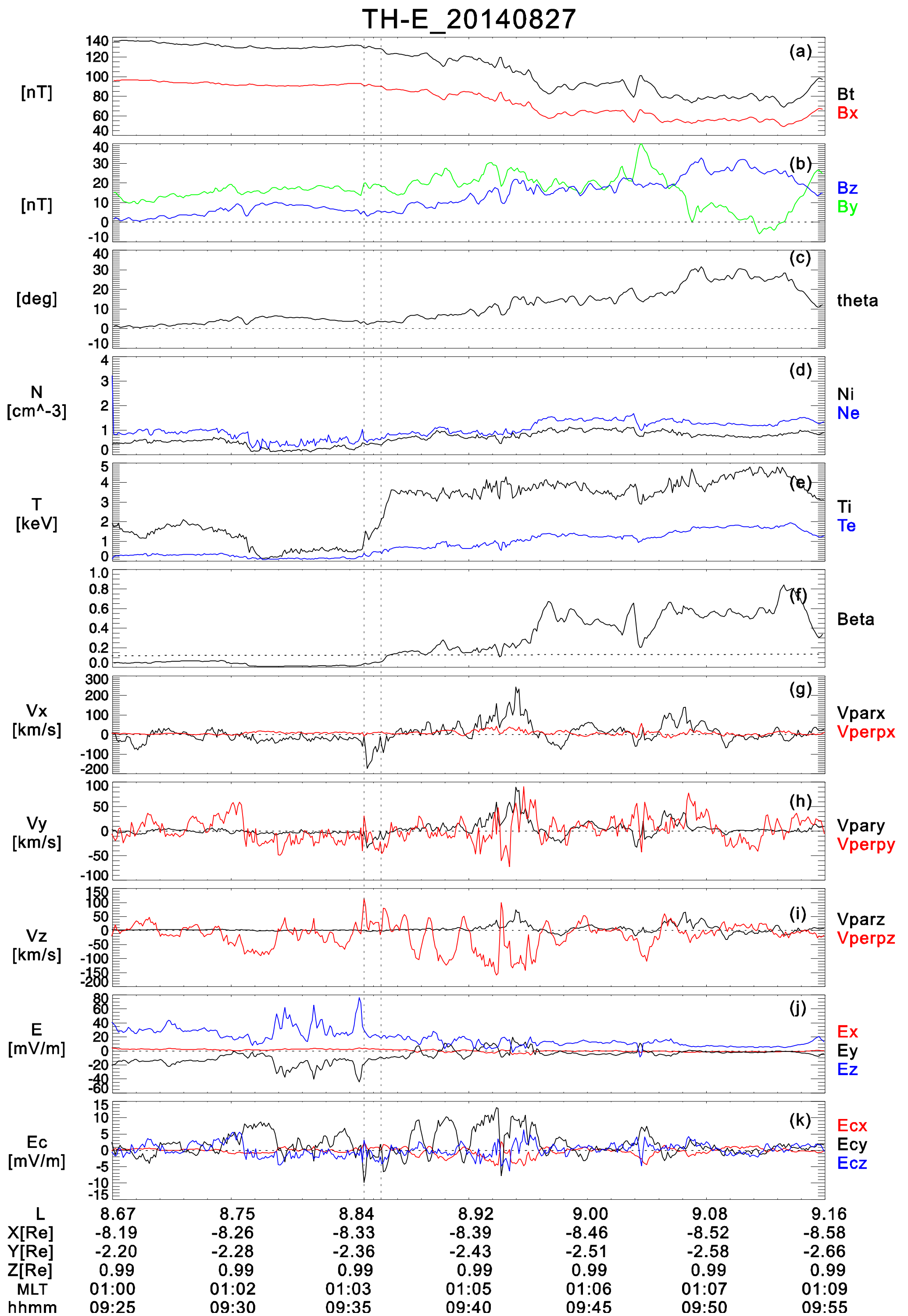
TH-E_20140827
[nT]
Bt
Bx
(a)
[nT]
Bz
By
(b)
[deg]
theta
(c)
N
[cm^-3]
Ni
Ne
(d)
T
[keV]
Ti
Te
(e)
Beta
(f)
Vx
[km/s]
Vparx
Vperpx
(g)
Vy
[km/s]
Vpary
Vperpy
(h)
Vz
[km/s]
Vparz
Vperpz
(i)
E
[mV/m]
Ex
Ey
Ez
(j)
Ec
[mV/m]
Ecx
Ecy
Ecz
(k)
L 8.67 8.75 8.84 8.92 9.00 9.08 9.16
X[Re] -8.19 -8.26 -8.33 -8.39 -8.46 -8.52 -8.58
Y[Re] -2.20 -2.28 -2.36 -2.43 -2.51 -2.58 -2.66
Z[Re] 0.99 0.99 0.99 0.99 0.99 0.99 0.99
MLT 01:00 01:02 01:03 01:05 01:06 01:07 01:09
hhmm 09:25 09:30 09:35 09:40 09:45 09:50 09:55

Figure 5

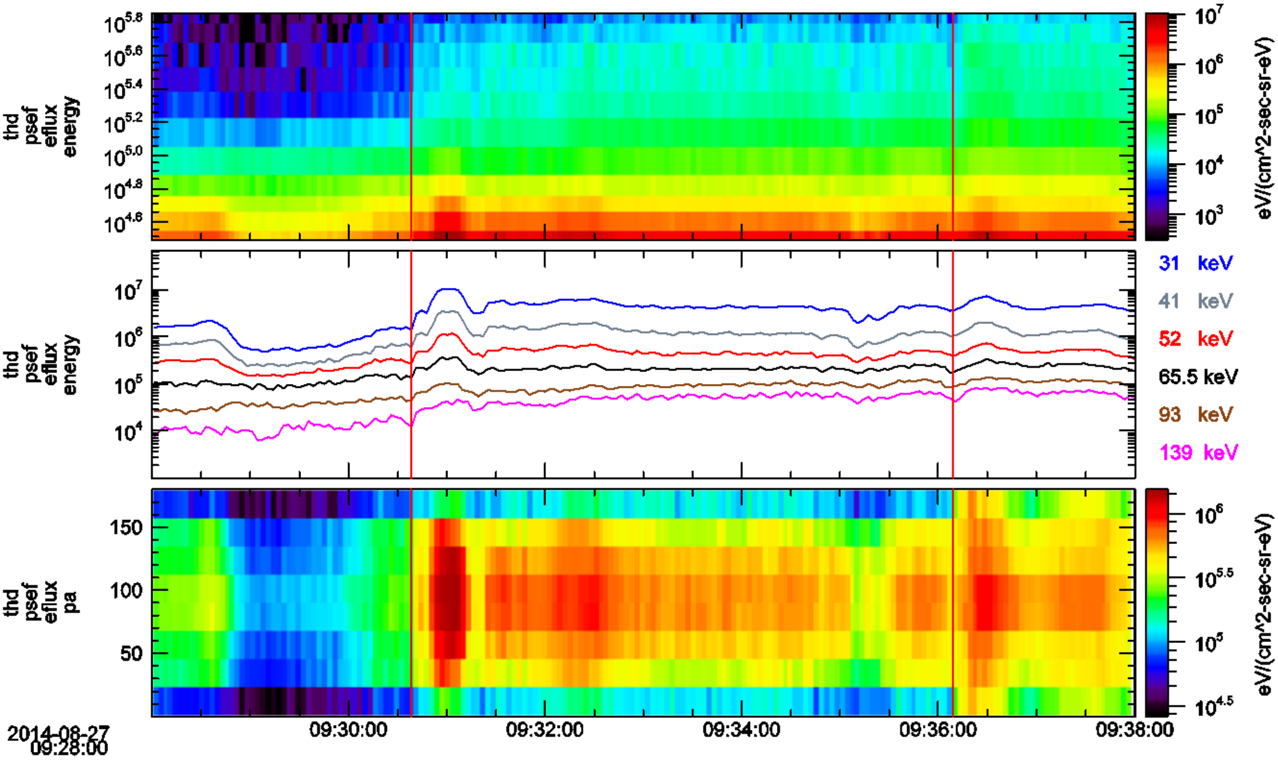
thd psef eflux energy
$10^{5.8}$
$10^{5.6}$
$10^{5.4}$
$10^{5.2}$
$10^{5.0}$
$10^{4.8}$
$10^{4.6}$
10^7
10^6
10^5
10^4
10^3
eV/(cm^2-sec-sr-eV)
thd psef eflux energy
31 keV
41 keV
52 keV
65.5 keV
93 keV
139 keV
thd psef eflux pa
150
100
50
10^6
$10^{5.5}$
10^5
$10^{4.5}$
eV/(cm^2-sec-sr-eV)
2014-08-27
09:28:00
09:30:00
09:32:00
09:34:00
09:36:00
09:38:00